



U.S. Department
of Transportation
**Federal Railroad
Administration**

Use of Dynamic Rail Deflection as a Means of Determining Changes in Top of Rail Friction

Office of Research and
Development
Washington, DC 20590

Notice

This document is disseminated under the sponsorship of the Department of Transportation in the interest of information exchange. The United States Government assumes no liability for its contents or use thereof.

Notice

The United States Government does not endorse products or manufacturers. Trade or manufacturers' names appear herein solely because they are considered essential to the objective of this report.

(blank page)

Table of Contents

EXECUTIVE SUMMARY	1
1.0 Introduction	3
2.0 Objectives	5
3.0 Test Site Overview	7
4.0 Traffic Overview	11
5.0 Data Collection.....	13
5.1 RDG Measurements	13
5.2 TPD Measurements	14
5.3 Tribometer Measurements/Event Log.....	14
6.0 Test Sequence.....	17
7.0 Data Analysis	19
7.1 Rail Deflection and Lateral Force Signal Characteristics	19
7.2 Spectral-Analysis of Raw RDG and L/V Signals.....	22
8.0 Correlation of Peak L/V and RDG Signals	25
8.1 RDG Analysis Software	25
8.2 RDG Measurement Site 1 (Soft Track, Co-Located TPD).....	25
8.3 RDG Measurement Site 2 (Stiffest Track, No TPD).....	28
8.4 RDG Measurement Site 3 (Stiff Track, Co-Located TPD)	29
8.5 RDG Measurement Site 4 (Softest Track, No TPD)	30
9.0 Suggested Equipment Improvements	33
Acronyms	35

(blank page)

List of Figures

Figure 1.	HTL Marked Up to indicate RDG Measurement Sites, TPD Sites, Lubricator Sites, and Running Directions	7
Figure 2.	RDG Installation at Section 25, Tie 199 (RDG Site 1, Co-Located with TPD)	9
Figure 3.	FAST Loop Lubrication Site in Section 24, with Gage Face Grease (High/Outside Rail) and TOR Oil (Low/Inside Rail) Applicator Bars Indicated	9
Figure 4.	Lubrication Site in Section 26, with Gage Face Grease (High/Outside Rail) and TOR Oil (Low/Inside Rail) Applicator Bars Indicated.....	10
Figure 5.	Sample (Raw) RDG Data showing Wheel Sensor (Blue), Low Rail (Red) and High Rail (Green) Signals—Wheel Sensor Values are in Volts, and Rail Deflection Signals are in Millimeters	14
Figure 6.	Low Rail Lateral Force Signal from 6.5-Degree Curve with Standard Cut-Tie Fasteners	19
Figure 7.	Example (Raw) RDG Signals from Site 1, showing Wandering Baseline due to Gross (Quasi-Steady State) Lateral Shifts	20
Figure 8.	Simplified Diagram Indicating External Forces Applied to the Rail Section, as well as the Internal Bending and Net Deflection Measured by the LVDT Probe	21
Figure 9.	FFT Magnitude Plots for Raw TPD (Left) and RDG (Right) Signals Taken at Measurement Site 3 (Stiff Track–Direct Fixation, Wood Ties).....	22
Figure 10.	FFT Magnitude Plots for Raw TPD (left) and RDG (right) Signals Taken at Measurement Site 1 (Soft Track–Cut Spikes, Wood Ties).....	23
Figure 11.	FFT Magnitude Plot for Raw and RDG Signal Taken at Measurement Site 2 (Stiff Track–Direct Fixation, Wood Ties).....	23
Figure 12.	FFT Magnitude Plot for Raw and RDG Signal taken at Measurement Site 4 (Soft Track–Cut Spikes, Wood Ties).....	24
Figure 13.	Average Lateral Forces and Deflections Calculated Per Lap	25
Figure 14.	Average Lateral Forces and Deflections Calculated Per Lap	25
Figure 15.	Correlation Between Average Lateral Forces and Deflections Calculated Per Lap .	26
Figure 16.	Correlation Between Average Lateral Forces and Deflections Calculated Per Lap .	26
Figure 17.	Scatter Plot of Peak Lateral Forces and Deflections Calculated Per-Axle	27
Figure 18.	Scatter Plot of Peak Lateral Forces and Deflections Calculated Per-Axle	27
Figure 19.	Average Lateral Forces and Deflections Calculated Per Lap	27
Figure 20.	Average Lateral Forces and Deflections) Calculated Per Lap	27
Figure 21.	Correlation Between Average Lateral Forces and Deflections Calculated Per Lap .	28
Figure 22.	Correlation Between Average Lateral Forces and Deflections Calculated Per Lap .	28
Figure 23.	Average lateral Forces and Deflections Calculated Per Lap.....	28
Figure 24.	Average Lateral Forces and Deflections Calculated Per Lap	28
Figure 25.	Correlation Between Average Lateral Forces and Deflections Calculated Per Lap .	29
Figure 26.	Correlation Between Average Lateral Forces and Deflections Calculated Per Lap .	29
Figure 27.	Average Lateral Forces and Deflections Calculated Per Lap	29

Figure 28. Average Lateral Forces and Deflections Calculated Per Lap	29
Figure 29. Correlation Between Average Lateral Forces and Deflections Calculated Per Lap .	30
Figure 30. Correlation Between Average Lateral Forces and Deflections Calculated Per Lap .	30
Figure 31. Average Lateral Forces and Deflections Calculated Per Lap	30
Figure 32. Average Lateral Forces and Deflections Calculated Per Lap	30
Figure 33. Correlation Between Average Lateral Forces and Deflections Calculated Per Lap .	31
Figure 34. Correlation Between Average Lateral Forces and Deflections Calculated Per Lap .	31

List of Tables

Table 1.	Descriptions of Measurement Test Sites.....	8
Table 2.	Tribometer Measurements and Event Log for Night 1 (6/6/2005-6/7/2005).....	15
Table 3.	Tribometer Measurements and Event Log for Night 2 (6/7/2005-6/8/2005).....	16

(blank page)

EXECUTIVE SUMMARY

To determine if the use of dynamic rail deflection (RDG) data can be used to determine the effectiveness of top of rail (TOR) systems, Transportation Technology Center, Inc. (TTCI) and Kelsan Technologies Corporation, with funding from the Federal Railroad Administration (FRA), engaged in a collaborative effort to assess the suitability of RDGs in assessing TOR friction modifier effectiveness. Phase I of the test plan, included in this report, involved testing at the FRA's Facility for Accelerated Service Testing (FAST) at the Transportation Technology Center (TTC), Pueblo, CO, using existing lubrication equipment to produce a range of lateral forces and correlate RDG response with truck performance detector (TPD) measurements.

Summary of Test Conduct and Preliminary Findings:

- Testing of a prototype RDG unit was conducted on the High Tonnage Loop (HTL) at FAST. RDG, TPD, and tribometer data were collected, allowing correlations to be established in range of track conditions. Data was collected at four measurement sites over two consecutive nights.
- Existing lubrication systems at FAST (high rail (HR) gage face grease/low rail (LR) TOR oil) were used to produce a range of rail friction patterns that altered truck curving performance and resulting lateral forces.
- Because the only variation during these periods of operation was rail friction, the intent was to evaluate the feasibility of RDG use in assessing the effectiveness of TOR friction control.
- Correlations between average values of peak lateral force and rail deflection (calculated for leading axles using a custom algorithm to remove nonlinear signal components) are strong, with R^2 values ranging from 0.83 to 0.99 where direct comparisons are possible. This suggests that rail deflection measurements are a valid way to assess TOR friction modifier performance, provided other variables are known and controlled.
- Deflection magnitudes were sufficient to provide good signal resolution across the range of track structures tested.
- Non-zero intercepts in the correlation equations suggest that the correspondence between percent reductions in lateral force and rail deflections will not be exact. It is expected that stiff track structures will perform better than soft structures in this regard. In addition, analysis of loaded cars will minimize the impact of non-zero intercepts via higher lateral forces and deflections in relation to the intercept values. This represents an opportunity for further improvement to the rail deflection analysis algorithms.

(blank page)

1.0 Introduction

The introduction of TOR friction modification is being considered by a number of railroads. A primary benefit from implementing TOR friction control is the reduction in lateral curving forces applied to the track from freight car trucks. Typically, reductions of 30 to 40 percent have been observed on a 5-degree curve from gage face (GF) only to GF + TOR.

Once applied, most TOR materials currently in use are invisible to the eye, taking the form of a very thin coating to the rail surface. Conventional methods used for measuring typical track lubrication (tribometer, rail temperature, and visual) are not always effective with TOR materials. Most evaluations of TOR systems at FAST and in the field have utilized strain-gage based load measurement stations. While such systems are accurate, they are expensive to install (\$10,000), require expensive equipment (valued at \$12,000+) to monitor loads, and are not portable. Should a nearby location become more appropriate for monitoring TOR effectiveness, the equipment must be relocated and another set of strain gages installed, at an additional cost of \$10,000.

To reduce the cost of field monitoring of TOR effectiveness, it has been proposed that measuring dynamic gage widening could provide a lower cost measurement method.

Limited demonstrations of a portable deflection system during TOR implementation have demonstrated performance suggesting that such an approach is viable. This was first observed at the FRA's FAST at TTC, Pueblo, CO, when railhead deflections using a static gage were noted to increase with increased curving forces. Currently FAST uses static gages to record the highest rail deflection during the passage of a train to alert wayside inspectors of higher than normal lateral loads. While these high deflections are generally associated with a bad acting car/truck, high deflections have also been observed when track lubrication changes to form a pattern leading to increased lateral loads.

Recent correlation work, conducted by Kelsan Technologies at several field sites where TOR friction control has been implemented, has shown that variations in TOR effectiveness can be seen in changes in dynamic gage widening. In addition, data from Norfolk Southern (NS) track geometry inspections has shown that, when operating over territories where TOR has been implemented, dynamic rail cant (railhead deflection or tipping) is reduced when compared to the immediate previous run.

To determine if the use of RDG data can be used to determine effectiveness of TOR systems, TTCI and Kelsan Technologies Corp. with funding from FRA, engaged in a collaborative effort to assess the suitability of RDGs in assessing TOR friction modifier effectiveness. Phase I of the test plan, included in this report, involved testing at FAST, using existing lubrication equipment to produce a range of lateral forces and correlate RDG response with TPD measurements (TPDs are strain-gage based lateral/vertical force measurement sites).

(blank page)

2.0 Objectives





Objectives for Phase I testing included:

- Install a prototype RDG unit (developed specifically for this work) at a number of locations on the HTL at FAST, representing a range of track conditions (structure, stiffness).
- Obtain data to facilitate a correlation between rail deflection (as measured by the RDG unit) and lateral forces (as measured by TPDs).
- Obtain data to examine the sensitivity of the RDG instrumentation with respect to the range of deflections seen under different track stiffness conditions.

This report describes testing undertaken at FAST during June 6-8, 2005.

(blank page)

Table 1. Descriptions of Measurement Sites

	Section (Tie No.)	Description	Picture
Site 1	25 (199)	6°L Cut Spikes Wood Ties Soft Track	 A close-up photograph of a railway track. The rails are connected by cut spikes. The track is supported by wooden ties. The track is set on a bed of gravel ballast. The number '200' is visible on the lower rail.
Site 2	25 (1319)	6°L Direct Fixation Wood Ties Stiffest Track	 A close-up photograph of a railway track. The rails are fixed directly to the wooden ties. The track is set on a bed of gravel ballast. A person's legs and feet are visible in the background.
Site 3	7 (306)	5°R Direct Fixation Wood Ties Stiff Track	 A wide-angle photograph of a railway track curving to the right. The track is supported by wooden ties. A white pickup truck is visible on the left side of the track. The track is set on a bed of gravel ballast.
Site 4	3 (522)	5°L Cut Spikes Wood Ties Softest Track	 A close-up photograph of a railway track. The rails are connected by cut spikes. The track is supported by wooden ties. The track is set on a bed of gravel ballast.

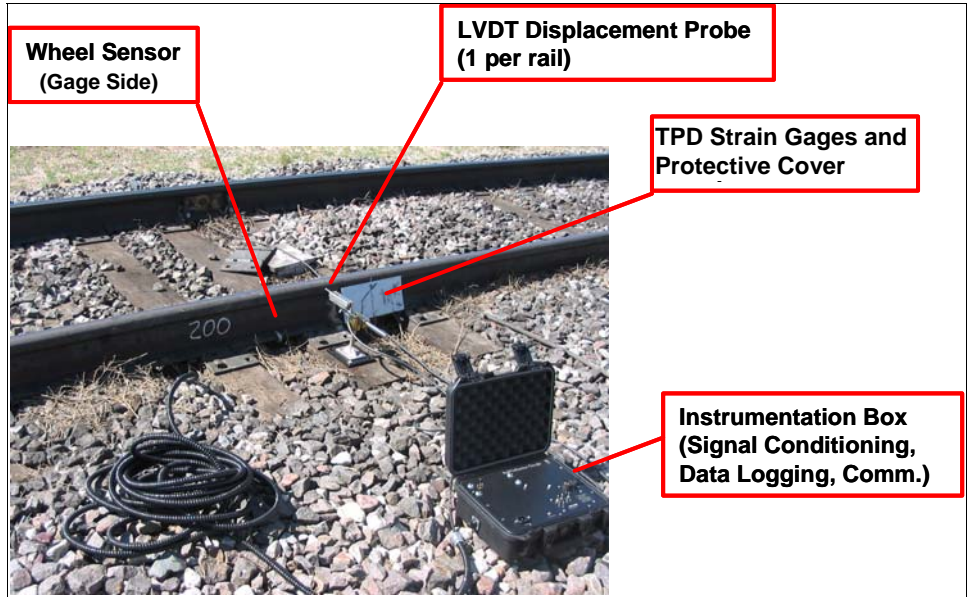


Figure 2. RDG Installation at Section 25, Tie 199 (RDG Site 1, Co-Located with TPD)

During testing at FAST, truck steering was manipulated through rail lubrication strategies to produce a range of lateral force levels. Specifically, two lubrication sites (shown in Figures 3 and 4) were used to control the application of grease on the outside rail GF and oil on the inside rail TOR.



Figure 3. FAST Loop Lubrication Site in Section 24, with Gage Face Grease (High/Outside Rail) and TOR Oil (Low/Inside Rail) Applicator Bars Indicated

As Figure 1 shows, the inside/outside rails correspond to the low/high rails in all curved sections except the reverse curve centered at Section 7. In this section, the lubrication strategy results in grease being applied on the low rail GF and oil on the high rail TOR.

In general, application of oil to the inside rail TOR surface was used as the primary control variable while grease application on the GF was held constant. Dry-down of the low rail TOR surface was used to generate high lateral forces through increased friction forces and anti-steering moments. Over application of oil to the top of the low rail (versus nominal running conditions) was used to create minimum lateral force levels. This can be done at FAST without detrimental side effects as the locomotives are not under full-tractive effort nor is train braking usually required. Such a lubrication pattern, even though it leads to reduced curving forces, is generally not recommended for revenue service application because of potentially detrimental side effects to tractive effort and braking related issues. When measuring deflections in Section 7, grease application was varied on the outside rail GF in an effort to produce a range of lateral forces. Variations in friction were produced using a variety of lubricants (grease and oil)—not friction modifiers. This was done to reduce costs and fit in with normal FAST lubrication policies, as past experience has shown that improperly adjusting these lubrication systems can lead to increased lateral curving forces. These changes in forces are due strictly to variations in friction as train speed, wheel/rail profiles, and other variables are kept constant.



Figure 4. Lubrication Site in Section 26, with Gage Face Grease (High/Outside Rail) and TOR Oil (Low/Inside Rail) Applicator Bars Indicated

4.0 TRAFFIC OVERVIEW

As Figure 1 shows, the HTL is a closed-loop test track. A single freight train runs on the track at a nominal speed of 40 mph, resulting in a complete lap occurring (approximately) every 4 minutes.

During the testing described here, four 4-axle diesel locomotives were configured at the head-end of a 78-hopper consist. All cars were loaded to 125 tons (62.5 kip axle load), resulting in a nearly uniform consist (some minor variability in hopper car bodies/trucks was present). This type of configuration is well suited to the evaluation of RDG instrumentation, as many variables (e.g., vertical load, car type, truck type, and wheel base) are held constant.

The running direction at FAST is typically alternated between clockwise (CW) and counterclockwise (CCW) directions to promote even wear of track components and remove effects associated with consistent directional running. During the testing described, the running direction was:

- Night 1 (6/6/2005-6/7/2005): CCW
- Night 2 (6/7/2005-6/8/2005): CW

These running directions were convenient as they were conducive to manipulation of lateral force levels at the RDG measurement sites. As Figure 1 shows, CCW running results in the train passing the lubricator at Section 24 just before RDG Measurement Sites 1 and 2. CW running results in the train passing this lubricator in advance of Measurement Sites 3 and 4.

(blank page)

5.0 Data Collection

As stated above, both RDG and lateral/vertical force (TPD) measurements were collected during testing at FAST. In addition, push-tribometer measurements of low rail TOR, high rail TOR, and high rail GF friction levels in (approximate) five-lap intervals were collected at the measurement sites to monitor the lubricated state of the rail as the lubrication strategy was adjusted to produce a range of lateral forces. The following paragraphs give a brief description of these measurements.

5.1 RDG Measurements

The prototype RDG (shown in Figure 2) collects rail deflection measurements through linear variable differential transformer (LVDT) based displacement probes, mounted such that the probe makes contact at the center of the vertical railhead surface on the field side. In addition, the signal from an active magnetic wheel sensor is used to trigger the system and track passing axles. Once triggered, the system collects data for a fixed period of time (corresponding to the maximum expected length of a single train), and then goes into a sleep mode until the subsequent train is detected.

All signals are collected by the RDG digital data acquisition system at a sampling frequency of 100 Hz, after passing through high order analog anti-aliasing filters with break frequencies tuned to 50 Hz.¹ Figure 5 shows a sample set of signals. The data shown was obtained at Measurement Site 2 (stiffest track). As shown, the stiff track structure results in clearly identifiable peaks in the rail deflection signal and a relatively stable zero point for each signal.

¹ As seen in Figures 9 through 12, spectral analysis of rail deflection signals at typical freight speeds has shown that the meaningful characteristic frequencies are typically less than 10 Hz.

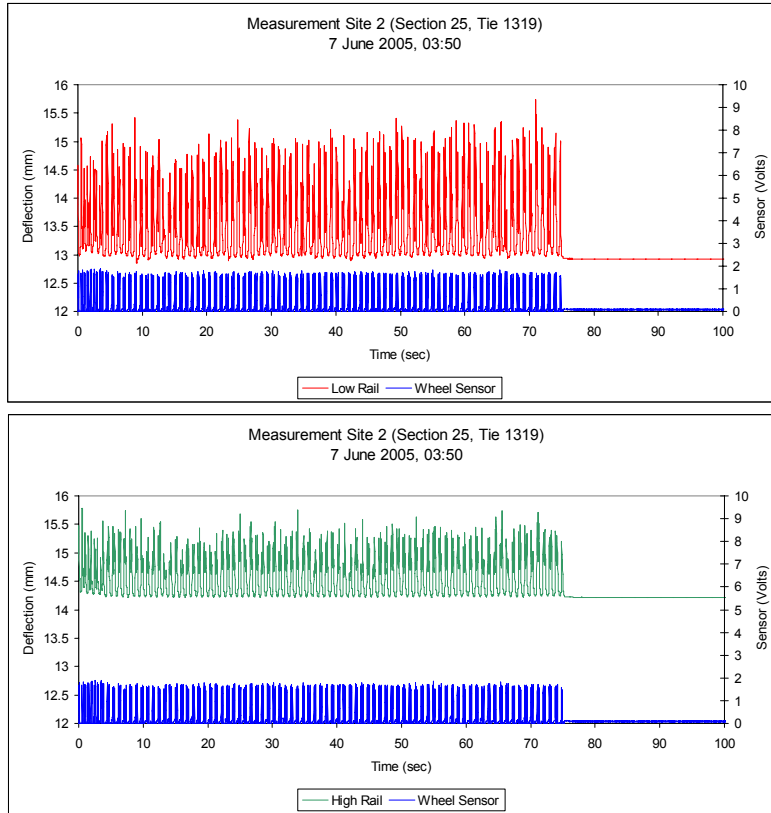


Figure 5. Sample (Raw) RDG Data showing Wheel Sensor (Blue), Low Rail (Red) and High Rail (Green) Signals—Wheel Sensor Values are in Volts, and Rail Deflection Signals are in Millimeters

5.2 TPD Measurements

Throughout testing, lateral/vertical force measurements were obtained via TPD sites. Measurement cribs 1/2 (Section 7), 3/4 (Section 9), and 5/6 (Section 25) were used to monitor and record lateral force levels. With data from RDG installations at Measurement Sites 1 and 3, a direct correlation with TPD signals is possible. For Measurement Sites 2 and 4, TPD data can be used to assess typical relative force levels for directional comparisons.

During testing, TPD data was plotted in quasi-real time (approximate two-lap lag) to assess in-track force levels and determine when each lubrication condition had reached steady state.

5.3 Tribometer Measurements/Event Log

Tables 2 and 3 detail tribometer measurements obtained during testing, as well as events and observations, such as changes in lubrication conditions and RDG re-location activities. Tribometer measurements were used to monitor the friction of each rail surface and provide further confirmation that changes in lubrication conditions were manifesting themselves in measured values of friction.

Table 2. Tribometer Measurements and Event Log for Night 1 (6/6/2005-6/7/2005)

Lap	Location	High Rail	Low Rail	Gage Face
1	Sec 25 Tie 199	46	48	
1	Lube on NORMAL			
5	Sec 25 Tie 199	36	37	25
10	Sec 25 Tie 199	37	33	21
12	Low Rail Oil OFF			
15	Sec 25 Tie 199	42	52	24
17	Low Rail Oil ON			
20	Sec 25 Tie 199	40	39	26
25	Sec 25 Tie 199	36	30	28
28	Low Rail Oil FLOOD			
30	Sec 25 Tie 199	34	28	18
35	Sec 25 Tie 199	43	26	40
38	Low Rail Oil OFF			
39	Low Rail Oil ON			
40	Sec 25 Tie 199	40	40	24
43-50	RDG Relocated to Sec 25, Tie 1319			
57	Sec 25 Tie 1319			
58	Low Rail Oil OFF			
65	Sec 25 Tie 1319	45	36	15
65	Low Rail Oil ON			
70	Sec 25 Tie 1319	43	42	17
72	LOW RAIL FLOOD			
75	Sec 25 Tie 1319	40	26	17
80	Sec 25 Tie 199	44	25	17
85	Sec 25 Tie 1319	29	32	18
86	Low Rail Oil NORMAL			
90	Sec 25 Tie 1319	32	33	17
96	Sec 25 Tie 199	35	30	12
96-102	RDG Relocated to Sec 7, Tie 306			
104	Sec 7 Tie 306	39	38	26
109	Sec 7 Tie 306	45	45	13

Table 3. Tribometer Measurements and Event Log for Night 2 (6/7/2005-6/8/2005)

Lap	Location	High Rail	Low Rail	Gage Face
1	Lube on NORMAL			
5	Sec 7 Tie 306	35	31	6
10	Sec 7 Tie 306	33	31	22
11	Track Lubrication at Steady State			
15	Sec 7 Tie 306	36	32	20
20	Sec 7 Tie 306	41	31	21
24	Low Rail Oil OFF			
26	Sec 7 Tie 306	35	33	29
29	Sec 26 Low Rail Oil ON			
30	Sec 7 Tie 306	40	33	29
32	Sanding Section 7			
33	Sanding Section 7			
35	Sec 7 Tie 306	35	49	33
40	Sec 7 Tie 306	37	39	25
42	Low Rail Oil ON			
45	Sec 7 Tie 306	47	28	30
49	Low Rail Oil FLOOD			
50	Sec 7 Tie 306	23	43	21
55	High Rail Grease FLOOD			
55	Sec 7 Tie 306	21	43	23
60	Sec 7 Tie 306	18	34	28
63	Sec 7 Tie 306	17	34	29
65	Low Rail Oil NORMAL			
67	High Rail Grease NORMAL			
70	Sec 7 Tie 306	20	36	20
74-82	RDG Relocated to Sec 3, Tie 522			
85	Sec 3 Tie 522	48	39	12
90	Sec 3 Tie 522	48	30	13
91	Low Rail Oil OFF			
95	Sec 3 Tie 522	48	38	11
97	Low Rail Oil ON			
100	Sec 3 Tie 522	39	32	12
105	Sec 3 Tie 522	44	32	9
108	Low rail oil FLOOD			
110	Sec 3 Tie 522	40	24	13
113	Low Rail Oil NORMAL, High Rail Grease OFF (Begin Dry-Down)			
115	Sec 3 Tie 522	29	22	12
117	Low Rail Oil OFF			
119	Sec 3 Tie 522	28	20	16
120	Sanding			
121	Sanding			
125	Sanding			
126	Sanding			
127	Sanding	50	47	29

6.0 Test Sequence

Four measurement sites were established for RDG testing on the HTL. Sites 1 (Section 25, tie 199) and 2 (Section 25, tie 1319) were monitored on Night 1 (6/6/2005-6/7/2005). Sites 3 (Section 7, tie 306) and 4 (Section 3, tie 522) were monitored on Night 2 (6/7/2005-6/8/2005). For each installation, the following general sequence was followed:

1. *Normal Forces*: Establish steady-state running with normal lubrication conditions (HR grease and LR oil applied at typical levels to balance forces) and collect at least five laps of data.
2. *High Forces*: Turn off LR oil, allowing the LR to dry-down and lateral forces to increase. This condition was maintained until maximum-deflection monitors (fish-scales) installed at key locations showed peak deflections approaching 0.5 inch. Following this, typical LR oil application was resumed.
3. *Normal Forces*: After returning to typical application levels, steady-state running was re-established (approximately five laps).
4. *Low Forces*: Over apply LR oil, flooding the rail and producing minimal lateral forces. At least five laps were collected before returning to normal conditions.
5. *Normal Forces*: After the low-force condition, LR oil was typically turned off for one to two laps and then turned on at normal levels to facilitate a rapid return to baseline conditions.

Deviations from the test sequence above occurred at Measurement Site 3 (Section 7, tie 306). As mentioned above, this is a reverse curve in which the lubrication strategy results in GF grease applied to the LR and TOR oil applied to the HR. As such, producing the desired range of forces was not straightforward. Combinations of reduced inside (high) rail oil application and over-application of outside (low) rail grease were attempted. While a range of lateral forces was produced, it was not as wide as the range seen at other sites.

In addition to the sequence above, a total dry-down was done in the final laps of Night 2 in anticipation of rail-flaw detector use on the following day. This provided additional data at Measurement Site 4 (Section 3, tie 522). As detailed in the observations listed above, outside rail GF grease was shut down at lap 113. Subsequently, inside rail oil was shut down at lap 117. Locomotive sanders were used on laps 120, 121, 125, and 126 to facilitate accelerated dry-down and provide extra data points.

(blank page)

7.0 Data Analysis

7.1 Rail Deflection and Lateral Force Signal Characteristics

As mentioned above, the purpose of this work is to assess the suitability of RDGs in assessing TOR friction modifier effectiveness. In particular, the aim is to examine the relationship between rail deflection and lateral force measurements to determine whether reductions in lateral forces can be correctly inferred from rail deflection data. For reference, Figure 6 shows a sample lateral force signal collected from a strain-gage based L/V measurement site installed in a 6.5-degree curve. As shown, distinct peaks in lateral force (corresponding to the passage of each axle) are seen, with a stable zero point continuing throughout the series of measurements.

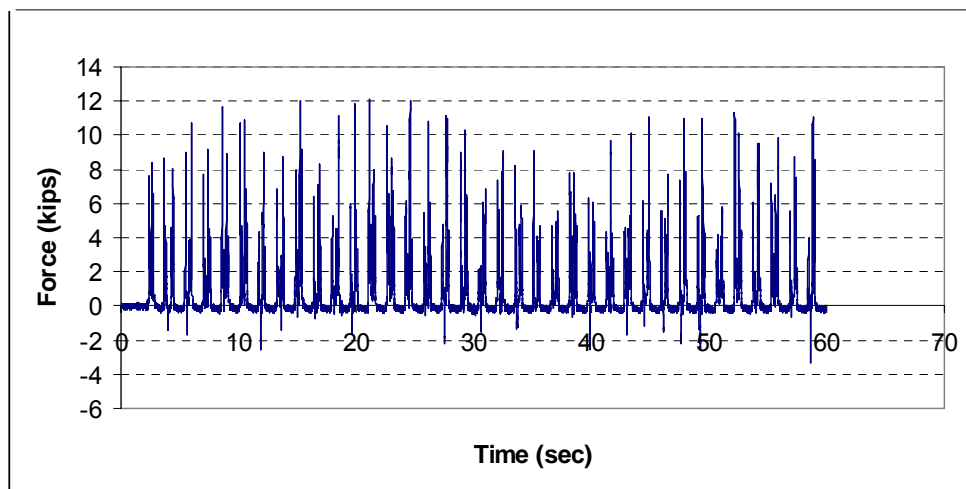


Figure 6. Low Rail Lateral Force Signal from 6.5-degree Curve with Standard Cut-Tie Fasteners

7.1.1 Dependence of Rail Deflection on Track Structure and Condition

As seen in Figure 5, rail deflection signals collected in stiff track structures have characteristics that are similar to those seen in lateral force measurements (Figure 6). Distinct peaks and a relatively stable zero point are seen in both signals.

In contrast, Figure 7 shows typical rail deflection signals collected at RDG Measurement Site 1 (Section 25, tie 199). As shown, gross shifts in the deflection signals are produced by quasi-static rail movements in this softer cut-spike track structure. These motions are accommodated by relative movement between the rail base and tie plate, and/or tie plate and tie. The presence of these gross shifts produces a wandering zero point, which makes analysis of dynamic rail deflection difficult.

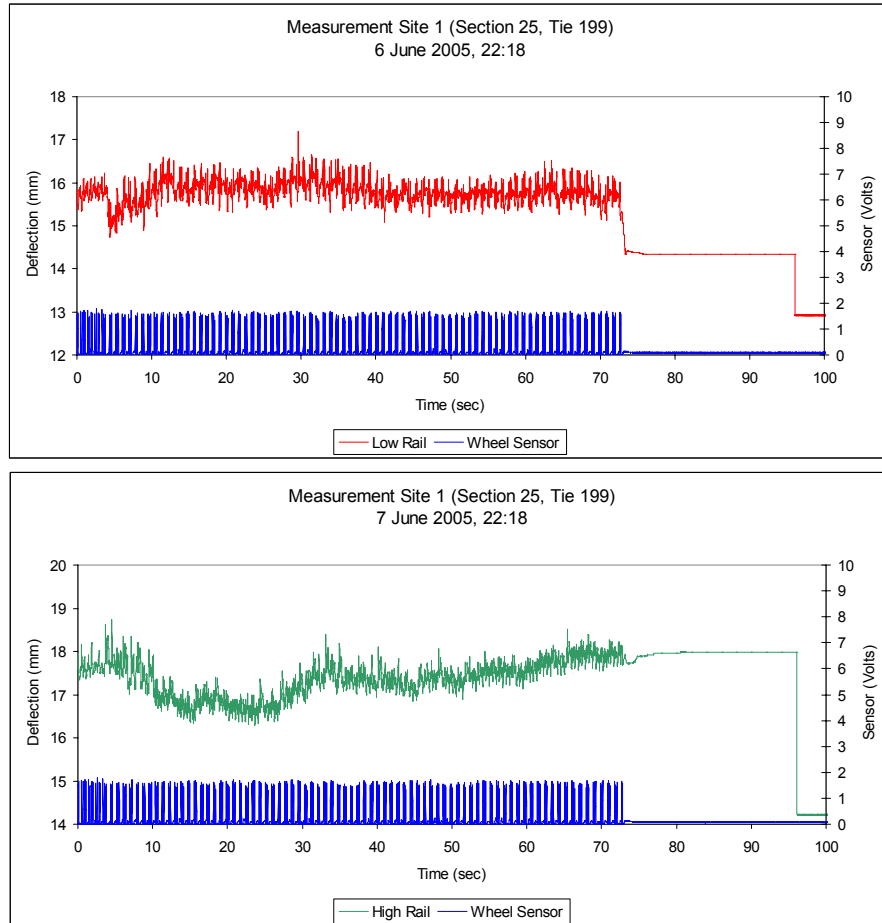


Figure 7. Example (Raw) RDG Signals from Site 1, showing Wandering Baseline due to Gross (Quasi-Steady State) Lateral Shifts

7.1.2 Dynamic Model of Rail Deflection

Figure 8 illustrates the external forces that are applied to the rail section with a passing wheel in a simplified way. In addition, the degrees of freedom and reaction forces occurring at both the rail base and tie plate are indicated. The internal bending of the rail is indicated by θ , and the net deflection measured by the LVDT probe is denoted by D .

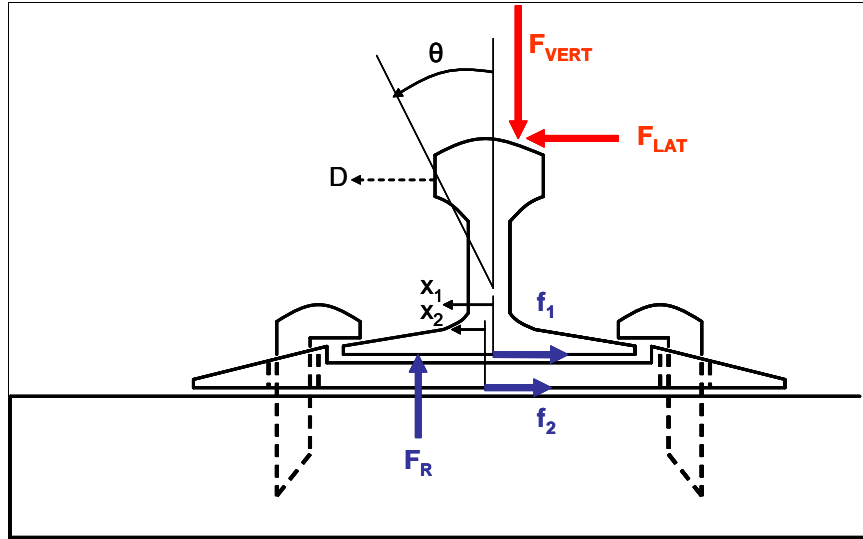


Figure 8. Simplified Diagram Indicating External Forces Applied to the Rail Section, as well as the Internal Bending and Net Deflection Measured by the LVDT Probe

F_{VERT} and F_{LAT} , the forces applied to the rail by the passing wheel, are dynamic forces that presumably reach a maximum value as the wheel is directly over the rail section. The lateral reaction force, f_1 , between the rail and tie plate will normally be a friction force that is linearly related to F_{VERT} through the nominal coefficient of friction at this interface and nonlinearly related to the relative velocity between the rail and tie plate ($\dot{x}_1 - \dot{x}_2$). The magnitude of f_1 will also be governed by the dynamic stiffness of the rail cross section. When the relative displacement between the rail and tie plate reaches the end of the available travel, f_1 will become a reaction force between the vertical surfaces of the rail and tie plate at the point of contact.

While the lateral reaction force f_2 is not applied to the rail, it is indicated in the figure because of its relation to relative motion between the tie plate and tie, which also appears in the net deflection signal, D . This reaction force is similar to f_1 in its relation to vertical load and the frictional characteristics between the tie plate and tie.

The vertical reaction force, F_R , at the bottom surface of the rail produces the required vertical force to balance the system based on the net moment created by the applied vertical and lateral forces, augmented by the lateral reaction force and dynamic stiffness effects.

Given the discussion above, a general dynamic model for the deflection of the railhead at the point of LVDT probe contact can be written (in the Laplace Domain) as:

$$D(s) \approx (d_1 + d_2) + G(s) \cdot F_{LAT}(s)$$

Where d_1 and d_2 are nonlinear, quasi-random gross shifts of the rail occurring at the rail/tie plate and tie plate/tie interfaces. The transfer function $G(s)$ maps the applied lateral force to a deflection term through the overall dynamic stiffness of the linear portion of the system. The typical form that would be expected for $G(s)$ is:

$$G(s) = \frac{1}{m_{eff} s^2 + c_{eff} s + k_{eff}}$$

where m_{eff} , c_{eff} , and k_{eff} are the effective mass, damping, and stiffness terms for the system, respectively.

Assuming that the data can be processed in a way that effectively removes the nonlinear gross rail movements, the resulting relationship between deflection and lateral force would be the given by the (approximately) linear:

$$D(s) \approx G(s) \cdot F_{LAT}(s)$$

If this is the case, then assuming that the underlying lateral force signals between measurement conditions are similar in frequency content on a bulk basis, a reduction in the average value of peak lateral force over a large number of axles will be accurately reflected in the reduction of the average value of the peak of the linear component of deflection.

7.2 Spectral-Analysis of Raw RDG and L/V Signals

In order to examine the relationship between RDG and L/V data empirically, a frequency domain (i.e., Fast-Fourier Transform (FFT) analysis) was performed on raw, time-series data from the TPD and RDG measurement sites.

7.2.1 FFT Comparison

Figure 9 shows the frequency spectra from TPD and RDG signals recorded at Measurement Site 3 (stiff track–direct fixation, wood ties). Lateral force and rail deflection signals are shown on the left and right of the figure, respectively.

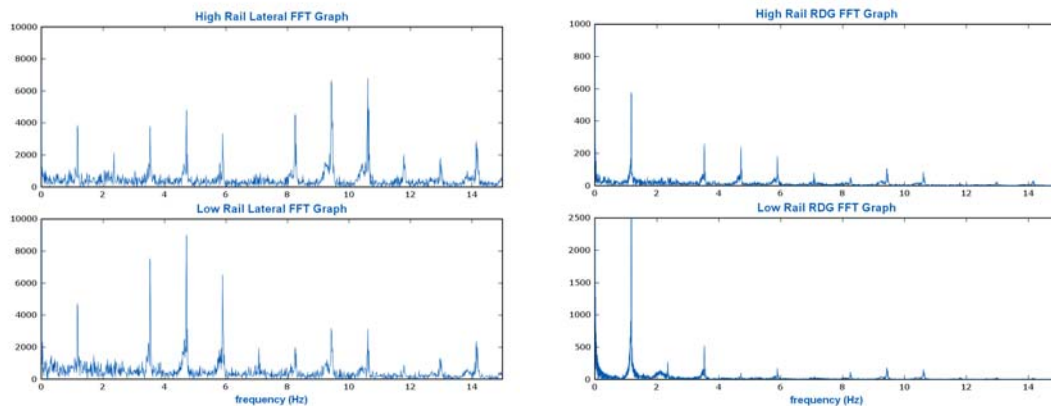


Figure 9. FFT Magnitude Plots for Raw TPD (Left) and RDG (Right) Signals Taken at Measurement Site 3 (Stiff Track – Direct Fixation, Wood Ties)

The fundamental frequency of ~ 1.2 Hz in both cases corresponds to the car-passing frequency (i.e., the basic periodicity of the train). As seen in the frequency spectra, both the L/V and RDG signals contain peaks at the same fundamental and harmonic frequencies. Higher frequency peaks in the RDG data are attenuated, as can be expected from the transfer function that maps lateral force to deflection.

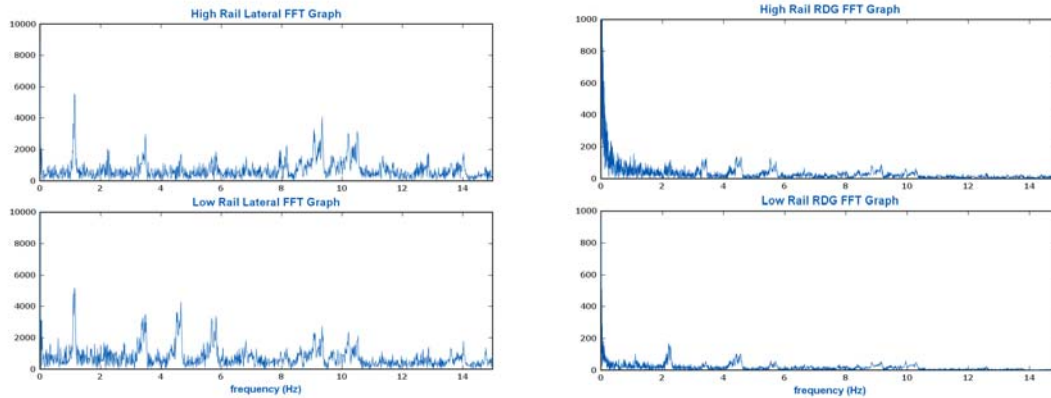


Figure 10. FFT Magnitude Plots for Raw TPD (Left) and RDG (Right) Signals Taken at Measurement Site 1 (Soft Track–Cut Spikes, Wood Ties)

Figure 10 shows the frequency spectra from TPD and RDG signals recorded at Measurement Site 1 (soft track–cut spikes, wood ties). In this case, the RDG spectra contain additional content at frequencies near and below the car-passing frequency. This corresponds to the nonlinear gross lateral shifts of the rail, as Figure 7 shows. The noise introduced by these shifts overlaps with the deflection data in the frequency domain. This further highlights the challenge in analysis of RDG data to produce meaningful results, particularly in soft track structures.

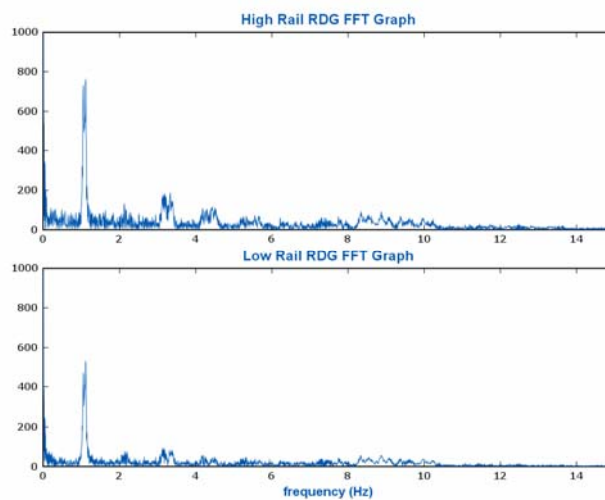


Figure 11. FFT Magnitude Plot for Raw and RDG Signal Taken at Measurement Site 2 (Stiff Track–Direct Fixation, Wood Ties)

Figures 11 and 12 show the RDG frequency spectra from Measurement Sites 2 and 4, respectively (recall that no TPDs are located at these sites). These plots further demonstrate signal content at the car passing frequency and harmonics, as well as low frequency noise that is more prevalent in softer track structures.

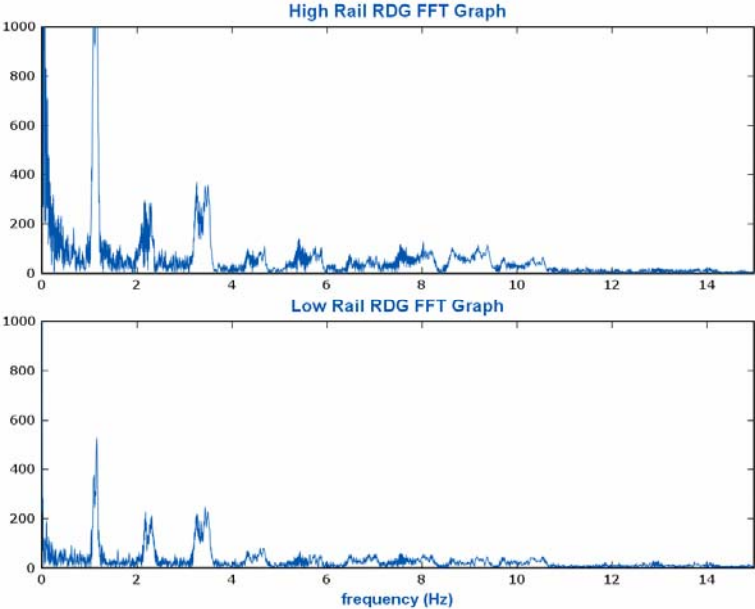


Figure 12. FFT Magnitude Plot for Raw and RDG Signal Taken at Measurement Site 4 (Soft Track–Cut Spikes, Wood Ties)

8.0 Correlation of Peak L/V and RDG Signals

8.1 RDG Analysis Software

Kelsan Technologies has developed a custom RDG signal analysis program. The RDG analysis software detects the peak deflection caused by each wheel and determines the corresponding axle type (leading/trailing truck, leading/trailing axle).

As mentioned above, one of the key requirements in analysis of rail deflection data is that the nonlinear portion of the signal be removed. Basic algorithms using the static rail position (obtained before/after each train) as a zero point have shown significant errors in estimation of dynamic deflection. With this in mind, Kelsan has developed an algorithm that estimates and updates the relaxed position of the rail with each passing car. The estimate is then used as the zero point when calculating peak deflections. This algorithm was used to generate the peak deflection data presented here.

8.2 RDG Measurement Site 1 (Soft Track, Co-Located TPD)

Figures 13 and 14 show the average values of peak lateral force and deflection calculated per lap at RDG Measurement Site 1. Each data point is the average value of force or deflection calculated for the 82-vehicle consist. Peak lateral forces were generated by TTCI and transmitted to Kelsan, while peak deflections were calculated using the algorithm described in the previous section.

Recalling that the LVDT probe was installed adjacent to TPD crib 5, the trend in average deflection can be seen to follow the trend in average lateral force closely, particularly following a break-in period associated with (approximately) the first 10 laps. It is possible that the rail response in the relatively soft cut-spike track structure adjusted as the rail temperature and lubrication conditions reached a stable running state.

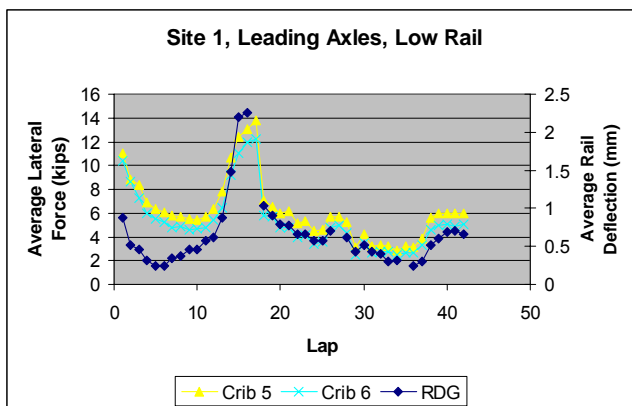


Figure 13. Average Lateral Forces and Deflections Calculated Per Lap

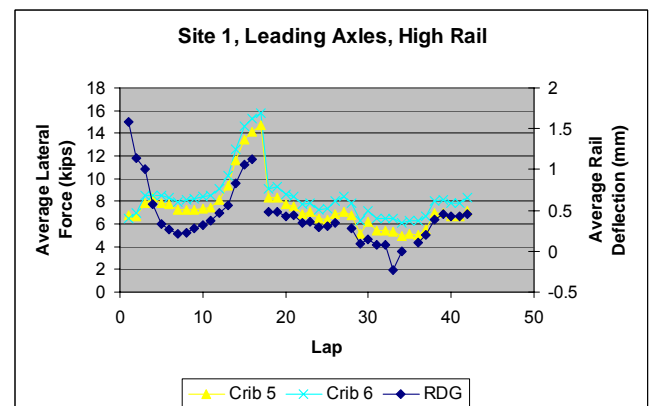


Figure 14. Average Lateral Forces and Deflections Calculated Per Lap

Figures 15 and 16 show the correlation between average values of peak lateral force and peak deflection, with the first 10 laps excluded. As shown, the correlation is strong with R^2 values of

0.93 and 0.89 for the low and high rails, respectively. The y-axis intercepts of 0.34 mm and 0.51 mm will result in an inexact correspondence between percent reductions in lateral force and deflection. The directional differences, however, will be highly consistent (suggesting that rail deflection may be considered a valid means to assess TOR friction modifier coverage/performance). In addition, analysis of loaded cars will minimize the impact of non-zero intercepts via higher lateral forces and deflections in relation to the intercept values. Further improvements in the rail deflection analysis algorithms may drive the intercept values closer to zero, improving the correspondence in estimates of percent change. The large data set created during this testing will aid in the validation of future algorithm enhancements.

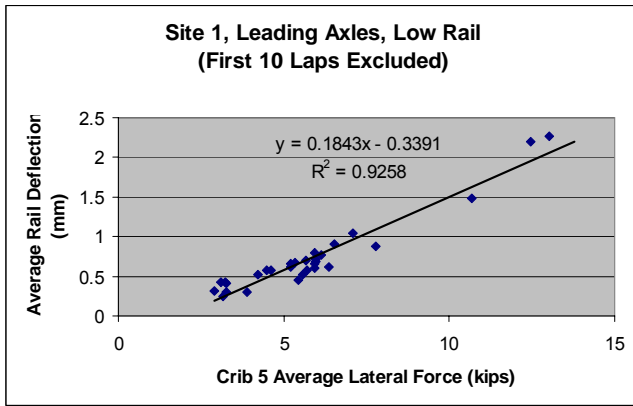


Figure 15. Correlation Between Average Lateral Forces and Deflections Calculated Per Lap

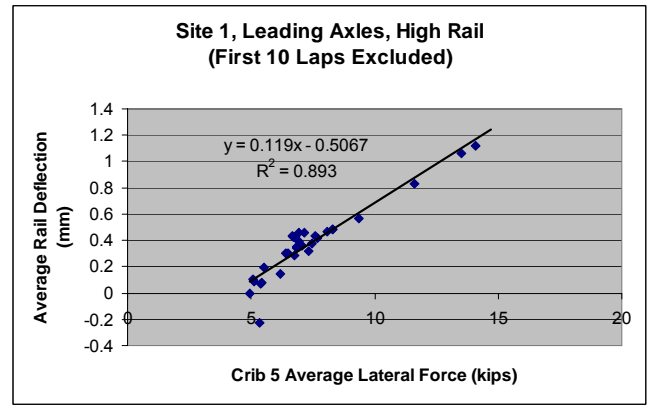


Figure 16. Correlation Between Average Lateral Forces and Deflections Calculated Per Lap

Figures 17 and 18 show scatter plots of peak lateral deflection versus force on a per-axle basis, calculated for both leading and trailing axles. While there is some scatter due to both the nonlinear components of rail deflection and variations in frequency content, the clear pattern reinforces the validity of the correlation between measurements.

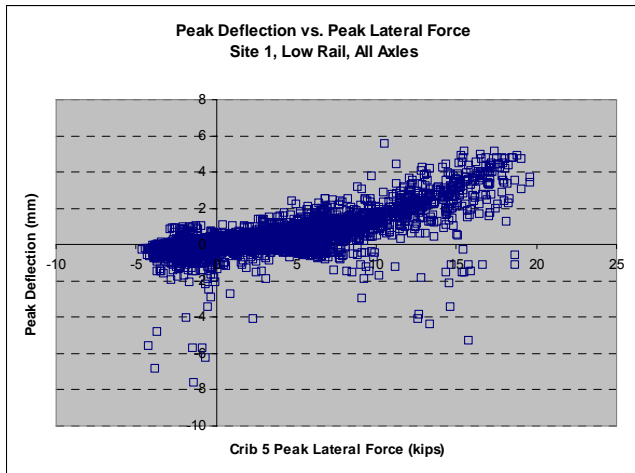


Figure 17. Scatter Plot of Peak Lateral Forces and Deflections Calculated Per Axle

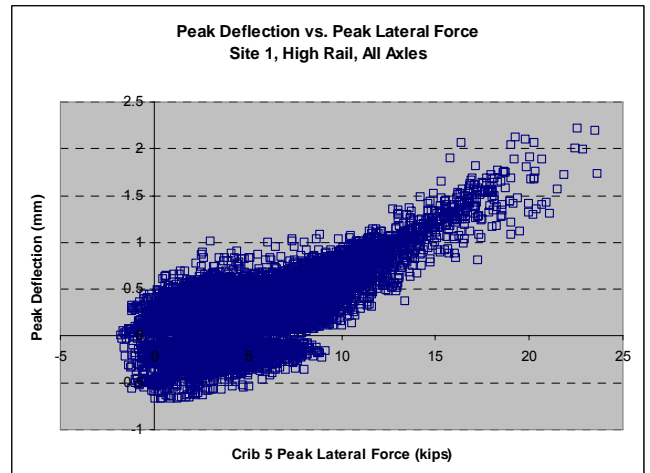


Figure 18. Scatter Plot of Peak Lateral Forces and Deflections Calculated Per Axle

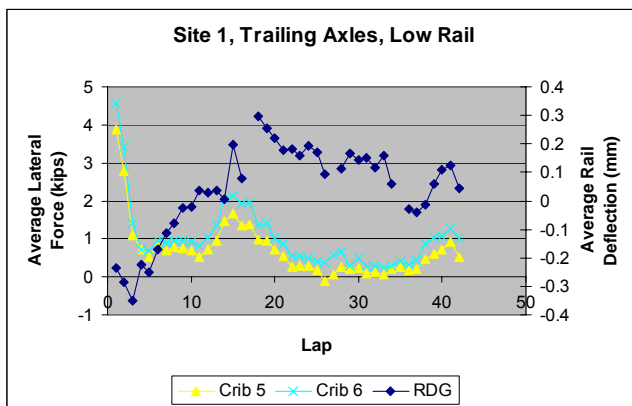


Figure 19. Average Lateral Forces and Deflections Calculated Per Lap

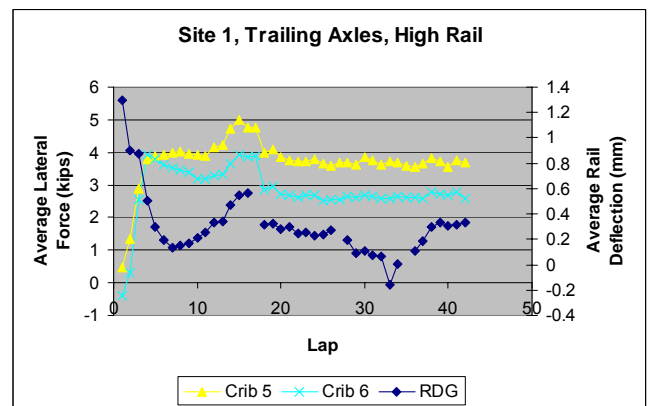


Figure 20. Average Lateral Forces and Deflections Calculated Per Lap

Figures 19, 20, 21, and 22 show the average values and correlations of peak lateral force and deflection collected at Measurement Site 1 for trailing axles. As shown, the correspondence between lateral force and deflection is much weaker than seen for leading axles. This is due to significantly lower lateral forces generated at the trailing wheelsets, reinforcing the focus on leading axles of loaded vehicles when interpreting rail deflection data.

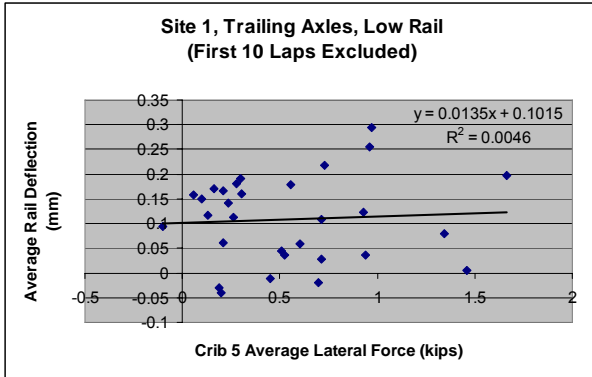


Figure 21. Correlation Between Average Lateral Forces and Deflections Calculated Per Lap

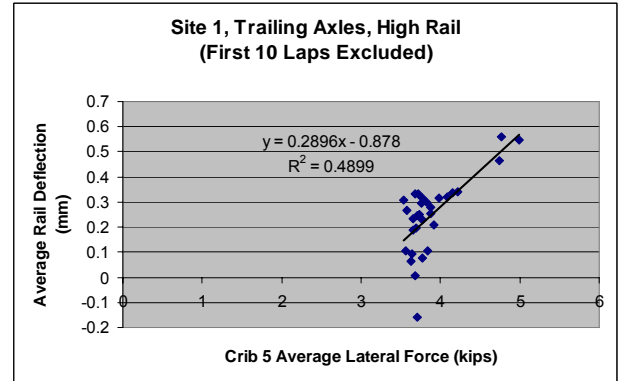


Figure 22. Correlation Between Average Lateral Forces and Deflections Calculated Per Lap

8.3 RDG Measurement Site 2 (Stiffest Track, No TPD)

Figures 23 and 24 show the average values of peak lateral forces at cribs 5/6 and peak deflection at RDG Measurement Site 2, calculated on a per lap (i.e., per-train) basis. Because the RDG and TPD measurement sites are not co-located in this case, lateral forces are not identical at both locations. Rather, lateral forces at cribs 5/6 can be seen as an indication of the directional trend in forces at the RDG measurement site. Despite the difference in physical location, the trend in average deflection can be seen to follow the trend in average lateral force closely. This is further supported by the correlations in Figures 25 and 26.

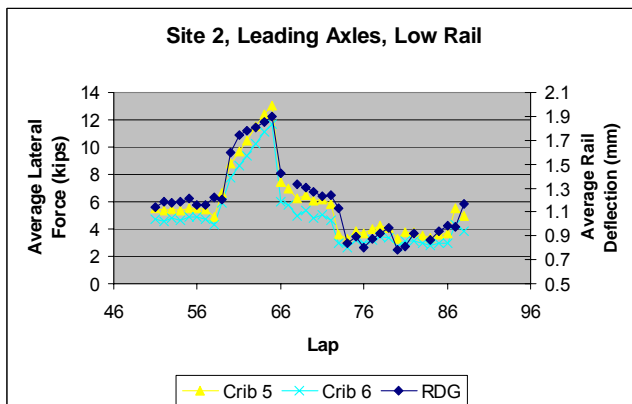


Figure 23. Average Lateral Forces and Deflections Calculated Per Lap

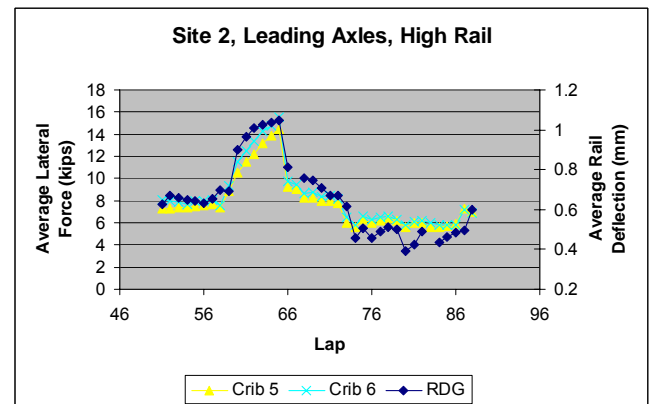


Figure 24. Average Lateral Forces and Deflections Calculated Per Lap

The range of peak deflections measured at this site (0.4–2.0 mm) is more than adequate for good signal resolution to be achieved via the RDG instrumentation. This indicates that RDG measurements are suitable in very stiff track structures. In addition, the clean signals shown in Figure 5 suggest that stiff track structures are more conducive for RDG measurements.

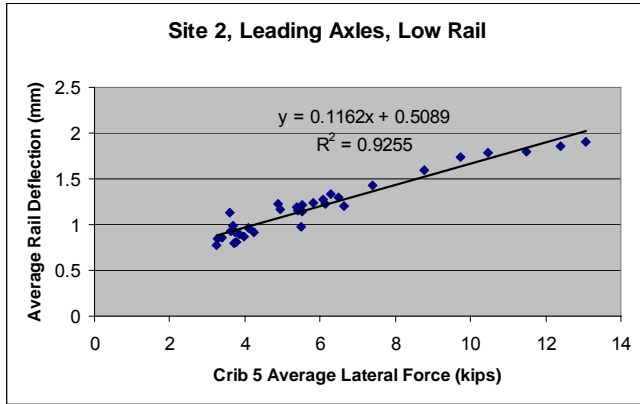


Figure 25. Correlation Between Average Lateral Forces and Deflections Calculated Per Lap

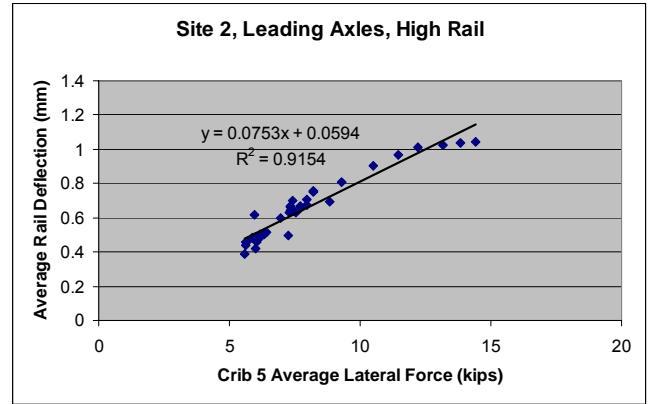


Figure 26. Correlation Between Average Lateral Forces and Deflections Calculated Per Lap

8.4 RDG Measurement Site 3 (Stiff Track, Co-Located TPD)

Figures 27 and 28 show the average values of peak lateral force and deflection calculated per lap at RDG Measurement Site 3.

Recalling that the LVDT probe was installed adjacent to TPD crib 2, the trend in average deflection can be seen to follow the trend in average lateral force closely. While a small separation does exist in the high rail signals, it must be reiterated that the range of lateral forces that was achieved at this site is small in comparison with Measurement Sites 1, 2, and 4 due to the impact of the reverse curve on the effectiveness of the lubrication strategy.

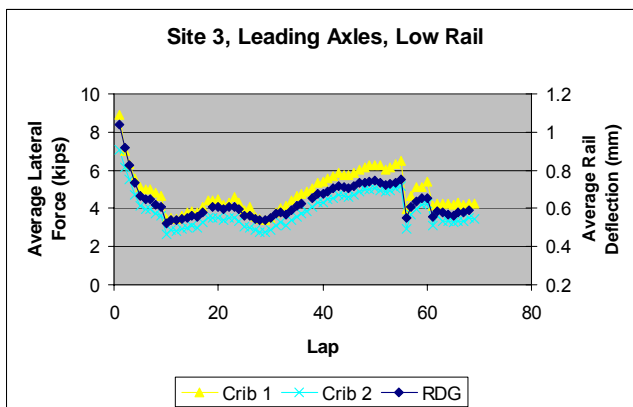


Figure 27. Average Lateral Forces and Deflections Calculated Per Lap

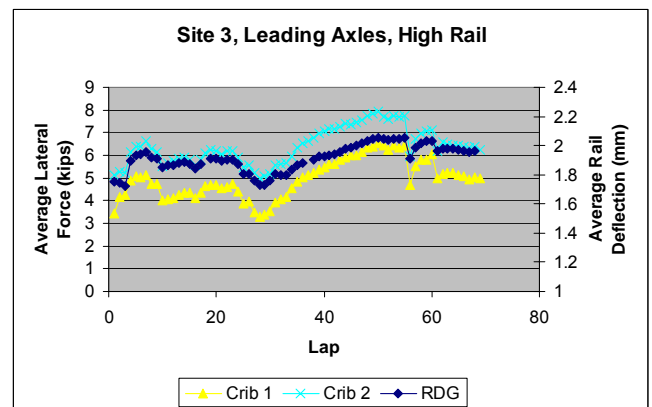


Figure 28. Average Lateral Forces and Deflections Calculated Per Lap

Figures 29 and 30 show the correlation between average values of peak lateral force and peak deflection. As shown, the correlation is strong with R^2 values of 0.99 and 0.83 for the low and high rails, respectively. The substantial high rail y-axis intercept is likely due to the limited range of lateral forces that was generated at this site.

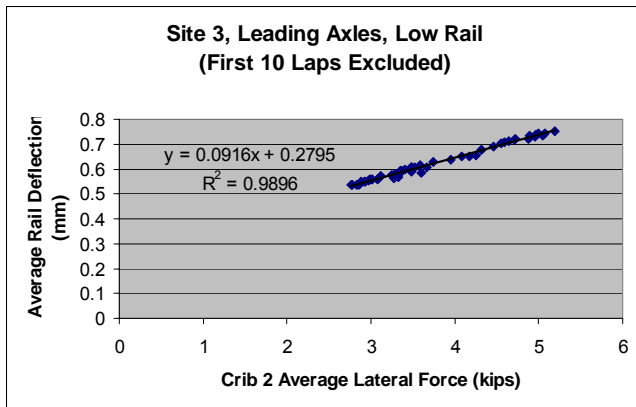


Figure 29. Correlation Between Average Lateral Forces and Deflections Calculated Per Lap

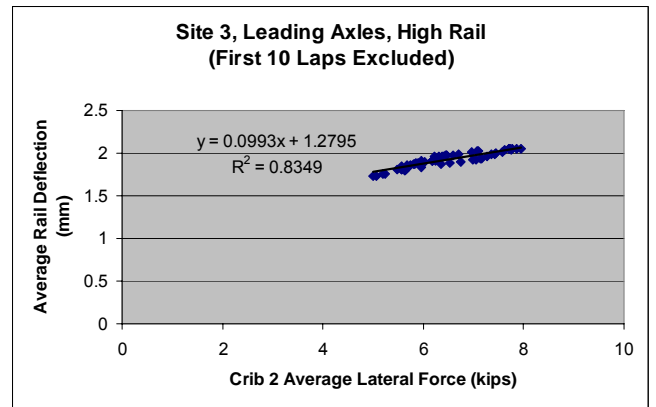


Figure 30. Correlation Between Average Lateral Forces and Deflections Calculated Per Lap

8.5 RDG Measurement Site 4 (Softest Track, No TPD)

Figures 31 and 32 show the average values of peak lateral forces at cribs 5/6 and peak deflection at RDG Measurement Site 4, calculated on a per lap (i.e., per-train) basis. In this case, the RDG and TPD measurement sites are located at a significant distance from each other (see Figure 1). As such, lateral forces at cribs 5/6 can be seen at best as an indication of the directional trend in forces at the RDG measurement site. Despite the difference in physical location and the very soft (i.e., highly nonlinear) track structure, the trend in average deflection can be seen to follow directional trend in average lateral force.

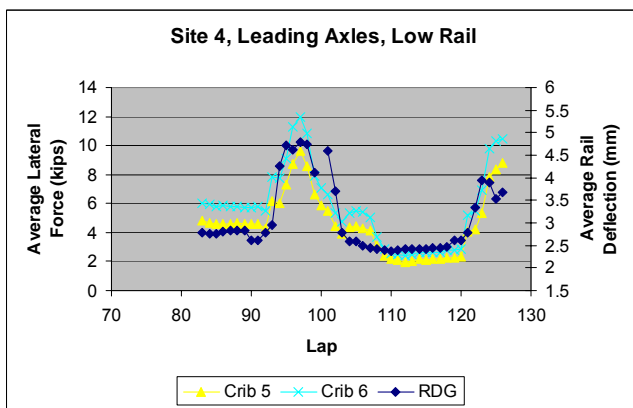


Figure 31. Average Lateral Forces and Deflections Calculated Per Lap

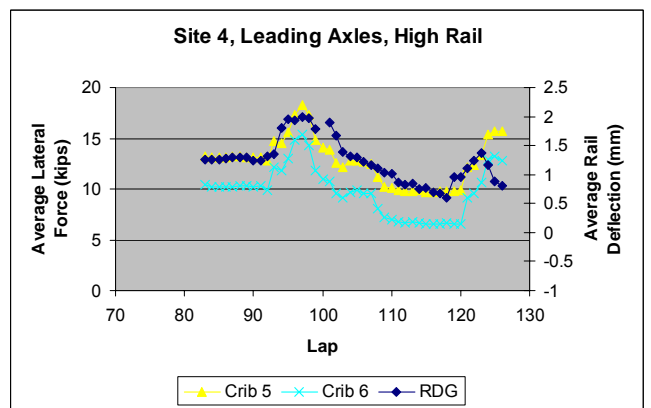


Figure 32. Average Lateral Forces and Deflections Calculated Per Lap

In addition to the basic directional agreement, the range of average rail deflections exhibited (1-5 mm) is reflective of the soft track structure. Raw data from this location shows substantial quasi-static shifts in rail location, which is in agreement with heavy plate cutting seen at the site.

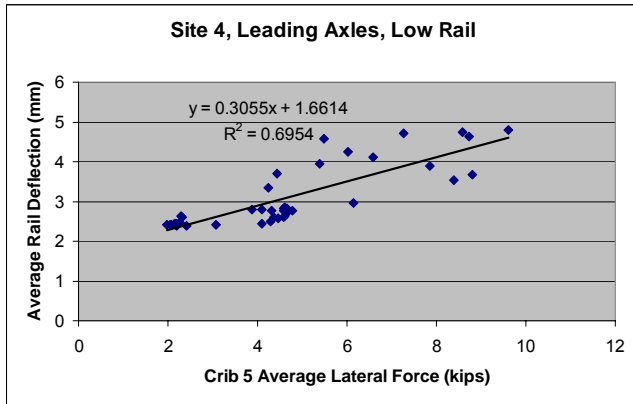


Figure 33. Correlation Between Average Lateral Forces and Deflections Calculated Per Lap

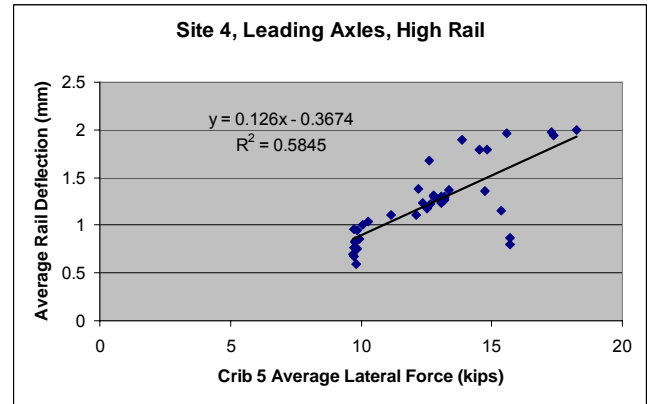


Figure 34. Correlation Between Average Lateral Forces and Deflections Calculated Per Lap

(blank page)

9.0 Suggested Equipment Improvements

After inspecting and installing the RDG prototype, field test personnel made a number of suggestions for equipment improvements, including:

- LVDT and wheel sensor cable-ends and connectors should be color-coded to ensure that incorrect connections are not made to the RDG instrumentation box.
- A set of magnetized calibration shims could be used to verify in-situ verification of displacement probe accuracy.
- LVDT cable lengths should be extended to allow RDG instrumentation box to be locked in an enclosure some distance from the track when using in areas where theft/vandalism is a risk.

In addition to these suggestions, Kelsan has identified several improvements that should be made as the prototype matures to a (potentially) commercial product, including:

- Revised internal layout (i.e., minor adjustments to top-plate machining) to enhance speed of assembly and ease of fit.
- Reduced internal hook-up wire diameter (gage) for enhanced compatibility with custom interface board terminal blocks.
- Adhesive application to any connectors without positive latching mechanisms to enhance resistance to vibrations.

As a follow up, a field demonstration on a revenue railroad with a variety of traffic will be conducted. This will allow data from a variety of trains operating over the same site to be evaluated. The site selected will be part of an existing heavy axle load monitoring site and is equipped with load detection equipment and wayside based TOR equipment. By varying the settings of the wayside TOR system, the effect on curving forces can be determined, along with the associated changes in RDG performance.

Provided acceptable results are obtained from the field test, a commercialization plan is planned to transition the RDG through the stage-gate process used at Kelsan and address any outstanding design issues. This will provide the railroad industry with an additional tool for use in assessing and adjusting TOR application systems in the field.

(blank page)

ACRONYMS

CW	clockwise
CCW	counterclockwise
FAST	Facility for Accelerated Service Testing
FFT	Fast Fourier Transform
FRA	Federal Railroad Administration
GF	gage face
HR	high rail
HTL	High Tonnage Loop
LR	low rail
LVDT	linear variable differential transformer
NS	Norfolk Southern
RDG	dynamic rail deflection
TOR	top of rail
TTCI	Transportation Technology Center, Inc. (the Company)
TTC	Transportation Technology Center (the Site)
TPD	truck performance detector

(blank page)